Scientia Iranica, Vol. 15, No. 5, pp 596–612

SCIENTIA
IRANICA

Application of a Kinematics-Driven Approach in Human Spine Biomechanics During an Isometric Lift

N. Arjmand[1], A. Shirazi-Adl[1,*], B. Bazrgari[1] and M. Parnianpour[2]

Effective prevention and treatment management of spinal disorders can only be based on accurate estimation of muscle forces and spinal loads during various activities such as lifting. The infeasibility of experimental methods to measure muscle and spinal loads has prompted the use of biomechanical modeling techniques. A major shortcoming in many previous and current models is the consideration of equilibrium conditions only at a single cross section, rather than along the entire length of the spine, when attempting to compute muscle forces and spinal loads. The assumption of extensor global muscles with straight rather than curved paths and of the spinal segments as joints with no translational degrees-of-freedom, are additional issues that need to be critically evaluated when simulating lifting tasks. The kinematics-driven approach, which satisfies equilibrium conditions in all spinal directions and levels and yields spinal postures compatible with external loads, muscle forces and nonlinear passive properties, while also taking into account the wrapping of trunk muscles, is employed. Results demonstrate that, regardless of the method used (optimization or EMG-assisted), single-level free body diagram models yield estimations that grossly violate equilibrium at other levels. The computed results are also markedly level-dependent. The crucial effects of the proper consideration of global muscles with curved paths and of spinal segments with translational degrees-of-freedom when attempting to estimate muscle forces and spinal loads in isometric lifting tasks are also demonstrated.

INTRODUCTION

Spinal disorders are the most prevalent cause of chronic disability in persons less than 45 years of age [1]. As many as 85% of the population in industrialized societies experience Lower Back Pain (LBP) that interferes with their work or recreational activities and, when surveyed, up to 25% of people between the ages of 30 to 50 years report lower back pain symptoms [2]. The total annual cost associated with LBP in the US alone has been estimated to range from between 20 to 50 billion dollars in 1992 [3]. In both prevalence and cost (treatment, absenteeism, compensation), Lower Back Disorders (LBDs) are, hence, recognized as being most significant [4,5].

LBP is very complex, with the exact source of the majority of cases remaining unknown. Nevertheless, mechanical factors are recognized in playing a prominent causative role in back injuries. Such events could occur both in a single episode during an accident or overload conditions and, over the course of time, with cumulative fatigue injuries. In a large survey, lifting or bending episodes accounted for 33% of all work-related back injuries [6]. The combination of lifting and lateral bending or twisting that occurs in asymmetric lifts has been identified as a frequent cause of back injury in the workplace [7-12]. Among various work-related activities, lifting, awkward posture and heavy physical work have been indicated to have a strong relationship with lumbar musculoskeletal disorders [13]. Several review studies on the epidemiology of LBP have concluded that lifting, in general, is one of the major documented risk factors for LBDs [14-16].

The foregoing studies on the association between heavy work and LBDs highlight the impor-

1. *Division of Applied Mechanics, Department of Mechanical Engineering, École Polytechnique, P.O. Box 6079, Station 'centre-ville', Montréal, Québec, Canada H3C 3A7.*
2. *Department of Mechanical Engineering, Sharif University of Technology, Tehran, Iran.*
*. *To whom correspondence should be addressed. E-mail: abshir@meca.polymtl.ca*

tance of biomechanical investigations of the human spine. Adequate knowledge of trunk muscle forces, spinal loads and spinal deformations, as well as the failure threshold of constitutive tissue under single and repetitive loading conditions, is essential in the establishing of safe-load and safe-motion limits in various recreational and occupational tasks. Prevention and treatment (non-surgical, surgical, rehabilitation) programs, sports medicine and performance enhancement regimens would benefit from a more accurate knowledge of muscle forces and spinal loads.

Currently, neither the loads (compression, shear, moments) on the human spine nor the forces in the trunk muscles can be measured directly by non-invasive approaches. Indirect estimation of muscle forces and spinal loads has been performed by measurement of, for example, Intra-Discal Pressure (IDP) [17,18], Intra-Abdominal Pressure (IAP) [19] and spinal shrinkage [20,21]. Controversies, however, exist as to the nature of assumptions needed to evaluate spinal loads from these indicators [22]. Cost and ethical (invasiveness) concerns have further limited the use of indirect measurements. The infeasibility of the direct quantification of muscle forces and spinal loads, as well as limitations in indirect measurement methods, has persuaded researchers towards the use of biomechanical modeling techniques.

Biomechanical Modeling Techniques

Biomechanical models have long been recognized as indispensable tools for the evaluation of spinal loads in various occupational and recreational activities. They use the basic principles of mechanics to estimate muscle forces and spinal loads. Forces in different active (i.e., trunk muscles) and passive (i.e., ligamentous spine) structures are calculated by satisfying the equilibrium between external moments, due to gravity/external loads, and internal moments produced by trunk active and passive structures, expressed at a particular spinal level (limiting ourselves to sagittaly symmetric and isometric cases by neglecting dynamic loads, as well as out-of-plane loads and movements shown in Figure 1):

$$\vec{r_{gr}} \times \vec{F_{gr}} + \vec{r_{\text{ext}}} \times \vec{F_{\text{ext}}} + \sum_{i=1}^{n} \vec{r_{abd}} \times \vec{F_{abd}} + \sum_{i=1}^{m} \vec{r_{bck}} \times \vec{F_{bck}} + \vec{M_p} = 0, \quad (1)$$

in which r_{gr}, r_{ext}, r_{abd} and r_{bck} are moment arms of gravity load (F_{gr}), external loads (F_{ext}), different (total of n) abdominal muscle forces (F_{abd}) and different (total of m) back muscle forces (F_{bck}), with respect to disc mid-height where the Free-Body Diagram (FBD) is considered, respectively. M_p is the passive moment resisted by the ligamentous spine, including disc, ligaments and facets at the segmental level of the FBD plane.

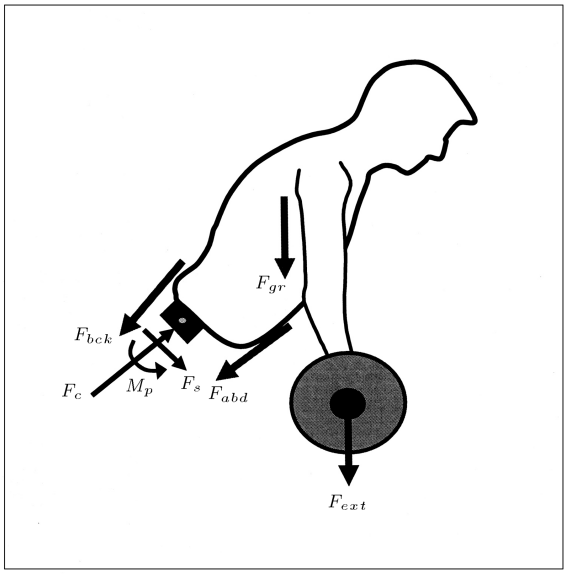

Figure 1. Free-body diagram to calculate spinal and muscle loads at a typical lumbar disc during lifting.

The moment of external loads ($r_{gr} \times F_{gr} + r_{\text{ext}} \times F_{ext}$) is usually estimated using a static or dynamic link segment model (for more details see [23]). M_p is generally estimated directly from the segmental rotation at the plane of the cut, using available moment-rotation properties (experimental or finite element studies). The equilibrium equation is solved to calculate unknown abdominal and back muscle forces. Once muscle forces are calculated, equilibrium can be employed in translational directions between external and internal forces, in order to compute axial compression and shear forces in local directions acting on the spine, as follows:

$$\vec{F_{gr}} + \vec{F_{\text{ext}}} + \sum_{i=1}^{n} \vec{F_{abd}} + \sum_{i=1}^{m} \vec{F_{bck}} + \vec{F_s} + \vec{F_c} = 0, \quad (2)$$

in which F_s and F_c are axial compression and anterior-posterior shear forces acting on the disc considered in this FBD.

The major problem in dealing with these equations is that Equation 1 cannot be solved deterministically, as the number of unknown muscle forces ($n+m$) exceeds that of available equilibrium equations (e.g., only one for the example in a sagittaly symmetric lift); i.e., the problem is highly redundant. Numerous biomechanical models for the estimation of spinal and muscle loads have, hence, been developed to tackle kinetic redundancy in the system of equilibrium equations. These can generally be grouped into four approaches; single-equivalent muscle, optimization-based, EMG-assisted, and kinematics-driven.

Single-Equivalent Muscle Approach

Earlier attempts to solve the redundancy problem have simplified the role of muscles by grouping them into synergistic ones, i.e., a single equivalent muscle represents all back muscles while ignoring abdominal ones [24-28]. This diminishes the number of unknown muscle forces, allowing for a unique solution to muscle forces and, subsequently, spinal loads. Obviously, this method fails to estimate forces in individual trunk muscles, including various fascicles of extensor back muscles, each of which attaches to a specific spinal level and which likely play a distinctive role during lumbar extension and lifting activities [29]. Besides, there is a wide range of data reported for the moment arm [29-34] and line of action [33,35,36] of the equivalent single muscle to which the predicted muscle and spinal load remain very sensitive [28,37].

Optimization-Based Approach

This is a very widely-used mathematical modeling approach to resolve kinetic redundancy, based on the assumption that there may be a single (or many) cost (objective) function (or functions) that could be minimized or maximized (optimized) by the Central Nervous System (CNS) while attempting to maintain equilibrium. Optimization was the first approach ever used to partition the moment of external loads between muscles in a multi-muscle model of the spine [38]. In this procedure, constraint equations on muscle forces are introduced, ensuring that muscle forces remain greater than zero and smaller than some maximum values corresponding to the maximum allowable stress of the muscles. Various linear and nonlinear cost functions have previously been used, the most common of which are based on a minimization of the intervertebral disc compression forces [38-41] and the sum of muscle stress to different powers [42,43]. In general, an optimization problem can be expressed as:

$$\text{Minimize (OF)} \quad \left(\text{e.g., OF} = \sum_{i=1}^{n} \left(\frac{F_i}{A_i} \right)^3 \right), \tag{3}$$

where the Objective Function (OF) is subject to the linear equality constraint corresponding to the following equilibrium equation:

$$\sum_{i=1}^{n} r_i \times F_i = M - M_P, \tag{4}$$

and the following inequality constraints (neglecting the passive muscle contribution):

$$0 \le F_i \le \sigma_{\max} \times \text{PCSA}_i, \tag{5}$$

where F_i, PCSA_i, $\sigma_{\max}$, n, r_i, and M denote the unknown total force in muscle i, the physiological cross-sectional area of the ith muscle, the maximum allowable active stress, the number of muscles cut by the FBD, the moment arm of the ith muscle and the moment of external loads, respectively. Note that Equations 1 and 4 are vectorial representations of equilibrium equations, accounting for the fact that the sagittal moment of the abdominal muscles opposes that of the extensor muscles. Naturally, in forward flexion tasks, in order to minimize the cost function considered in Equation 3, the optimization procedure assigns no forces to abdominal (antagonistic) muscles. The inability of optimization approaches to predict the activity of antagonistic muscles is recognized as one of the major shortcomings of this approach. The co-contraction of antagonist muscles, however, has been introduced in the optimization approach by assuming a non-zero lower bound for muscle forces in Equation 5 [44]. The lack of a physiological basis for the assumption that CNS operates in accordance with a specific cost function to partition loads among muscles, as well as the deterministic nature of optimization-based recruitment predictions, despite the presence of inter and intra-individual variabilities in performance, are other deficiencies of this approach [23,45]. Nevertheless, optimization methods are still the most common approaches used to estimate individual muscle forces in mathematical models of various joints [46].

Predicted muscle forces, using an optimization approach, are qualitatively validated by comparison with the measured EMG activity of muscles. Cost functions, whose predictions for muscle forces correlate with measured muscle activation, are considered adequate [42,43,47,48]. A multi-criteria cost function, in which the sum of weighted cost functions is simultaneously optimized, has also been proposed, in order to circumvent the problem associated with the single cost function of the minimization of either axial compression acting on the spine or intervertebral displacements, which yield muscle activities in disagreement with EMG data [49].

EMG-Assisted Approach

In the light of foregoing criticisms of the optimization approach, the use of electromyography (EMG) collected from trunk muscles has been advocated to derive a biologic solution to the redundancy present in biomechanical models [50-52]. Muscle contractions accompany electrical signals that could be measured by surface electrodes on the skin overlying the muscle or by fine wire electrodes penetrated deep inside the muscle. In order to estimate force in trunk muscles, a relationship between the EMG activity of trunk muscles and their force is presumed. Obviously, calculating muscle forces in this way will not necessarily assure the satisfaction of equilibrium equations (Equation 4). Therefore, a gain factor, to which all

calculated muscle forces are multiplied, is introduced to satisfy equilibrium conditions. The EMG-assisted method is given credit for its ability to predict force in antagonistic muscles and for its sensitivity to inter and intra-individual variabilities.

Apart from the difficulty in simultaneously recording the activity of all existing muscle fascicles, a limitation of EMG-assisted modeling is the inaccessibility of deep muscles by superficial electrodes, which are often used as a measure of activity in these muscles. One must use intra-muscular wire electrodes to measure the activity of deeper muscles, as recent in vivo studies have reported that the deep and superficial fibres of trunk muscles are controlled independently [53]. Nevertheless, appropriately located surface EMG electrodes may adequately represent the amplitude of deeper muscle activities for a variety of tasks [54].

Even for larger flat muscles, the EMG activity is measured from one site of the muscle, despite the existing regional differences in muscle activity [55-58]. Besides, controversy exists regarding the nature of relations between muscle forces and associated EMG activity. Due to these difficulties, the EMG-assisted approach has been described as being cumbersome [59], or even impossible [60], for the precise prediction of muscle forces in terms of both data acquisition and EMG-force relationships. The use of gain as a unique value in all muscles, which could vary when considering equilibrium in another plane, is another source of concern.

To improve the accuracy of predictions, a hybrid optimization-EMG based model has been suggested [61,62]. The objective of this newer version is to maintain equilibrium in different planes by applying the least possible adjustments to individual muscle forces. In other words, individual gain factors were calculated for muscles. It was concluded that using such a hybrid approach would improve predictions when compared with collected EMG data [61].

Kinematics-Driven Approach

Since this method is employed in the current work, it will be presented, in detail, in a subsequent section.

Common Shortcomings

A major shortcoming in many current and earlier biomechanical model studies of multi-segment spinal structure lies in the consideration of the balance of net external moments only at a single cross section (typically at lowermost lumbar discs) (see Figure 1) rather than at different levels along the entire length of the spine [38,50,62-66]. These models are widely employed in ergonomic applications and in injury prevention and treatment programs. It has been indicated, though without detail, that the muscle forces evaluated, based on such single-level equilibrium models, once applied on the system, along with external loads, may not necessarily satisfy equilibrium at remaining levels along the spine [67]. The extent of violations in equilibrium at different levels and their effects on the estimated muscle forces and spinal loads, however, have not yet been quantified.

To overcome the foregoing shortcoming, linear finite element models, along with optimization algorithms, have been developed and used to evaluate muscle recruitment, internal loads and a stability margin [49,67-70]. A simplified geometrical model of the spine with rotational degrees-of-freedom and nonlinear stiffness properties, along with the EMG-assisted approach, has also been employed to evaluate muscle forces and the stability margin in various tasks [35]. The translational Degrees-Of-Freedom (DOF) at various joints and, hence, the associated shear/axial equilibrium equations, were totally neglected in this latter model, which may adversely influence predictions on muscle forces and system stability [67].

Proper considerations of the nonlinear material properties of the thoraco-lumbar motion segments in different directions with load and direction-dependent properties, with the realistic distribution of gravity/external loads and with verification of the stability using nonlinear analysis, are important in obtaining reliable results. Adequate nonlinear representation of a passive spine, particularly in the presence of large compression forces and flexion rotations expected in lifting tasks [71-73], is important not only in the proper partitioning of the net moments among passive-active components, but also in the stability analysis of the system. Besides, realistic consideration of spinal geometry and deformation under loading is crucial in the proper determination of both active and passive spinal loads, as well as spinal stability.

Wide ranges of data have been reported in the literature for the Lever Arm (LA) of Erector Spinae (ES) in the sagittal plane ($\sim 4-8$ cm) [29-34], as well as for their Line Of Action (LOA) [33,35,36]. Both the lever arm of ES [74-76] and the angle between their LOA and the longitudinal axis of vertebrae [75,77] have been observed to decrease as the spine flexes forward in the sagittal plane. The extent of such alterations, especially for thoracic fascicles of the ES, needs yet to be determined [75]. A crucial issue is the accurate consideration of the pathway of local (i.e., with upper attachments at lumbar vertebrae) and global (i.e., with upper attachments at the rib cage) ES muscles. Unlike during upright postures, in which these pathways may accurately be assumed as straight lines between insertion points, such may not be assumed in tasks involving large lumbar flexions. In latter tasks, a straight line assumption for global muscles could violate kinematic constraints by penetrating

into intervening hard/soft tissues. The local lumbar muscles have been suggested not to take significantly curved orientations in flexion [75]. Curved rather than linear pathways should, however, be considered for global muscles, especially in tasks involving large trunk flexion, if the precise estimation of muscle forces and spinal loads is sought. Some earlier biomechanical models [35] considered curved pathways for extensor muscles, which pass through several points at different vertebrae. These models, however, appear to have failed to account for reaction (contact) forces at these points of contact between muscle and vertebra. These contact forces are due to changes in muscle orientation and generate moment as well as shear/compression forces that need to be considered in associated equilibrium equations at different levels. The simulation of wrapping without the proper consideration of these contact forces at the deformed configuration of the spine is not, hence, adequate, which adversely affects the accuracy of estimations.

The objective of the current work is, therefore, to apply the kinematics-driven approach, which guarantees the satisfaction of equilibrium conditions at all spinal levels, while considering both the nonlinear material properties of the thoraco-lumbar motion segments and the wrapping of trunk thoracic extensor muscles around the vertebrae. Moreover, under an isometric lifting task, the extent to which the computed muscle/spinal loads and equilibrium requirements at different levels are influenced by a Single-Level Free Body Diagram (SLFBD) model, by neglecting translational degrees-of-freedom at different levels and, by assuming a straight line of action (rather than curved paths) for trunk extensor muscles, is quantified.

MATERIALS AND METHODS

In vivo study: Fifteen healthy males with no recent back complications volunteered for the study after signing an informed consent form. Their mean age, body height and mass were 30 ± 6 years, 177 ± 7 cm and 74 ± 11 kg, respectively. While bending slightly forward, infrared light emitting markers, LED, were placed on the tip of the spinous processes at T1, T5, T10, T12, L1, L3, L5 and S1 levels. Three extra LED markers were placed on the ilium (left/right iliac crests) and posterior-superior iliac spine for the evaluation of pelvis rotation and one was placed on the bar to detect the position of weights in the hands. A three-camera Optotrak system (NDI International, Waterloo/Canada) was used to collect 3D coordinates of LED markers. For the sake of the validation of model predictions for the muscle forces, EMG signals were recorded bilaterally over the following trunk muscles [78,79]: Longissimus dorsi ($\sim$ 3 cm lateral to midline at the L1), iliocostalis ($\sim$6 cm lateral to midline at the L1), multifidus ($\sim$ 2 cm lateral to midline at the L5), external obliques ($\sim$ 10 cm lateral to midline above umbilicus and aligned with muscle fibres) and rectus abdominis ($\sim$ 3 cm lateral to midline above the umbilicus). The raw EMG signals were collected at 1500 Hz, amplified, band-pass filtered at 10-400 Hz by a 2nd order Butterworth filter and rectified. The RMS was then calculated over a 4s trial duration and averaged for both sides. For normalization, EMG data at a Maximum Voluntary Contraction (MVC) was collected in standing (in cardinal planes while loaded via a strapped harness [80]), prone and supine positions.

The subjects were handed a load of 180 N in the front, via a long bar, when in an upright standing posture and when flexing the trunk forward by $\sim 46^\circ$ with knees straight in the sagittal plane. During tests, subjects were instructed to keep arms extended in the direction of gravity. The total trunk and pelvis rotations, relative to the upright standing posture, were computed. Pelvis rotation was computed by tracking the orientation of 'normal' to the plane passing through the three markers on the pelvis. Total lumbar rotation was computed as the difference between the thorax and pelvis rotations [81].

Thoracolumbar Finite Element Model

A sagittally-symmetric T1-S1 beam-rigid body model [82-85], comprised of 6 deformable beams to represent T12-S1 discs, 7 rigid elements to represent T1-T12 (as a single body) and lumbosacral vertebrae (L1 to S1), was used (Figure 2). The beams modeled the overall nonlinear stiffness of T12-S1 motion segments (i.e., vertebrae, disc, facets and ligaments) at different directions and levels. The nonlinear load-displacement response under single and combined axial/shear forces and sagittal/lateral/axial moments, along with the flexion versus extension differences, were represented in this model, based on the numerical and measured results of previous single- and multi-motion segment studies [83,84,86,87]. Based on the authors recent studies [72], the stiffness of the motion segments during sagittal rotation was further modified to account for the stiffening effect observed in the presence of moderate to large compression loads [71,73]. The insertion points of beams to rigid vertebrae were shifted posteriorly from the end-plate centers by 4 mm to account for posterior movement in the disc axis of rotation observed under loads in different directions [88,89]. In all cases, a gravity load of 387 N was considered and distributed eccentrically at different levels from T1 to L5 vertebrae [90,91]. The weight of 180 N was applied at the location measured in vivo via a rigid element attached to the T3 vertebra.

For the flexed posture, the mean measured trunk (46°) and pelvic (16°) rotations were prescribed on the T12 and S1 levels, respectively. As for the individual lumbar vertebrae, the total lumbar rotation (30°) was partitioned in accordance with proportions reported in earlier investigations [87,92-95] and prescribed at individual segments (8% at T12-L1, 13% at L1-L2, 16% at L2-L3, 23% at L3-L4, 26% at L4-L5 and 14% at L5-S1 levels).

A sagittaly-symmetric muscle architecture with 46 local (attached to lumbar vertebrae) and 10 global (attached to thoracic cage) muscles, having, initially, straight Lines Of Action (LOAs) in a neutral standing posture, was used [29,30,33] (Figure 2 and Table 1). To simulate curved paths in forward flexion tasks, global extensor muscles were assumed to wrap around the vertebrae. The wrapping contact at each T12-L5 level was assumed to occur only when the instantaneous lever arm distance at that level decreased below either 100% or 90% of its corresponding value in the neutral standing posture.

To evaluate muscle forces, a novel kinematics-driven algorithm (Figure 3) was employed to solve the redundant active-passive system under prescribed measured kinematics and external loads [84,85,96]. Prescribed rotations at different spinal levels generate an equilibrium equation at each level, in the form of $\sum r_i \times f_i = M$ (r: Muscle lever arm, f: Muscle force and M: Required sagittal moment due to the prescribed rotation). Each prescribed kinematic on the spine provides an additional equilibrium equation between unknown muscle forces and external loads; thus, decreasing the degree of redundancy of the system. If the number of equilibrium equations at a particular spinal level reaches that of unknown muscle forces, the problem would be solved deterministically. Such an approach not only satisfies the equilibrium equations in all directions along the entire length of the spine, but yields spinal postures in full accordance with external/gravity loads, muscle forces and passive tissue with nonlinear properties. To resolve the existing redundancy, an optimization algorithm, with the cost function of the sum of the cubed muscle stresses, was employed along with the inequality equations of unknown muscle forces remaining positive and greater than their passive force components (calculated based

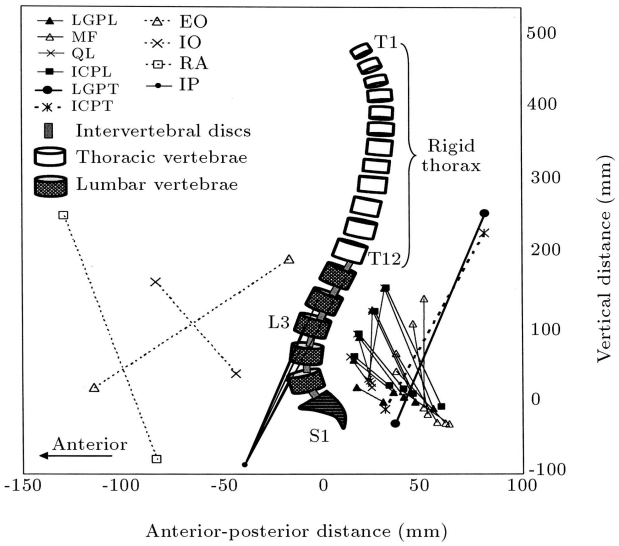

Figure 2. The FE model as well as global and local musculatures in the sagittal plane (only fascicles on one side are shown) in upright standing posture at initial undeformed configuration. ICPL: Iliocostalis Lumborum pars lumborum, ICPT: Iliocostalis Lumborum pars thoracic, LGPL: Longissimus Thoracis pars lumborum, LGPT: Longissimus Thoracis pars thoracic, MF: Multifidus, QL: Quadratus Lumborum, IP: Iliopsoas, IO: Internal Oblique, EO: External oblique and RA: Rectus Abdominus (axes are not to the same scale).

Table 1. Pysiological Cross Sectional Area (PCSA, mm^2) and initial length (in brackets, mm) for muscles on each side of the spine at different insertion levels.

Local Muscles	ICPL[a]	IP[b]	LGPL[c]	MF[d]	QL[e]
L1	108 (170)	252 (276)	79 (172)	96 (158)	88 (137)
L2	154 (118)	295 (241)	91 (132)	138 (135)	80 (104)
L3	182 (84)	334 (206)	103 (88)	211 (106)	75 (74)
L4	189 (50)	311 (169)	110 (52)	186 (82)	70 (46)
L5	-	182 (132)	116 (25)	134 (51)	-
Global Muscles	**RA[f]**	**EO[g]**	**IO[h]**	**ICPT[I]**	**LGPT[J]**
T1-T12	567 (353)	1576 (239)	1345 (135)	600 (250)	1100 (297)

(a) ICPL: Iliocostalis Lumborum pars lumborum; (b) IP: Iliopsoas;

(c) LGPL: Longissimus Thoracis pars lumborum; (d) MF: Multifidus;

(e) QL: Quadratus Lumborum; (f) RA: Rectus Abdominus; (g) EO: External Oblique;

(h) IO: Internal Oblique; (I) ICPT: Iliocostalis Lumborum pars thoracic;

(J) LGPT: Longissimus Thoracis pars thoracic.

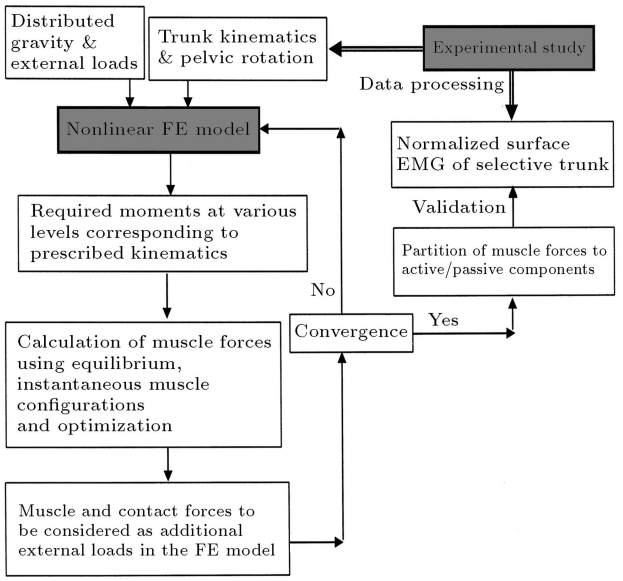

Figure 3. Flow-chart for the application of the kinematics-driven approach and determination/validation of trunk muscle forces and spinal loads.

on muscle strain and a tension-length relationship [97]), but smaller than the sum of the maximum physiological active forces (i.e., 0.6× physiological cross-sectional area, PCSA) plus the passive force components [98].

To simulate curved paths in forward flexion tasks, the global muscles (i.e., thoracic iliocostalis and longissimus) were assumed to wrap around pre-defined points that were located on and moved with T12-L5 vertebral levels. During the iterative analyses, the wrapping contact at each T12-L5 level occurred only when the instantaneous lever arm distance at that level decreased below its corresponding (critical) value in the neutral standing posture being 58, 56, 56, 56, 52 and 44 mm for global iliocostalis and 53, 53, 55, 56, 54 and 48 mm for global longissimus at T12, L1, L2, L3, L4, and L5 vertebral levels, respectively. In these cases, no reduction in the LA distances was, hence, allowed, as the trunk flexed from the upright posture. To investigate the likely effect of alterations in these critical LA values set for the beginning of the contact on results, an additional case under a trunk flexion of 46° was also studied, assuming 10% smaller critical LAs. Nonlinear finite element formulation of the curved paths was performed, based on earlier work on the modeling of wrapping elements [72,99,100]. The wrapping reaction forces at each T12-L5 level were calculated at each iteration of the analysis by application of the equilibrium at instantaneous deformed configurations taking identical muscle force in adjacent segments (i.e., frictionless contact). These wrapping reaction forces, along with the axial and shear force penalties of the calculated muscle forces, were fed back into the finite element model as additional updated external loads. This iterative approach was continued until convergence was reached.

Single-Level Free Body Diagram (SLFBD) Model

Under the final deformed configurations of the ligamentous spine, local and global wrapping muscles and muscle forces, as well as gravity/external load magnitudes/locations identical to those in the previous kinematics-driven cases, were re-calculated, based on a Single Level Free Body Diagram (SLFBD) equilibrium at different (L5-S1 through T12-L1) intervertebral disc mid-planes, expressed as follows:

$$\sum_{i=1}^{n} r_i \times f_i = M_{\text{ext}} - M_{\text{passive}},$$

in which n, M_{ext}, and M_{Passive} denote the number of all muscle fascicles crossing the cutting plane under consideration, the total net external moment due to gravity and the external load carried in the hands and the passive ligamentous resistant moment at that level, respectively. The passive ligamentous moments at different levels were taken exactly as those calculated in the kinematics-driven models at the final deformed configurations. Unknown muscle forces were subsequently evaluated by the same optimization algorithm used in the reference models (i.e., sum of cubed muscle stresses). Spinal compression and shear forces at different levels were then computed by consideration of the equilibrium in local axial and shear (anterior-posterior) directions.

In order to examine whether or not the muscle forces estimated, based on the SLFBD model at the L5-S1 level, verify the equilibrium at the remaining levels, the calculated muscle forces at this level were applied onto the Free Body Diagrams (FBDs) at each of the remaining L4-L5 through T12-L1 levels. An Index of Equilibrium Violation (IEV), defined below, was computed at each of these levels:

$$\text{IEV}\% = \frac{(M_{\text{muscles}} + M_{\text{passive}}) - M_{\text{ext}}}{M_{\text{ext}}} \times 100,$$

in which M_{muscle}, M_{Passive} and M_{ext} denote moments at the disc level under consideration, generated by muscle forces calculated based on SLFBD equilibrium at the L5-S1 level, the passive ligamentous spine and the gravity/external load carried in the hands, respectively. This index, IEV, represents, hence, an indication of the extent of moment equilibrium violation at different levels when applying the muscle forces estimated at the L5-S1 level.

Furthermore, based on the same muscle forces, axial compression forces at the upper T12-L5 levels

were also computed and compared at each level with their respective value estimated, based on the SLFBD performed at that level rather than at the L5-S1 level. In this case, the index of error signifies the relative difference between the estimated axial compression at each level when the SLFBD model is performed, either at the distal L5-S1 level or at that particular level. It is to be re-iterated that the geometry of the spine and muscles for both loading cases used in the SLFBD models is taken as being identical to that in the final deformation of the corresponding reference cases evaluated, based on the kinematics-driven models.

Finally, for the task of an upright standing posture with a load in the hands, the muscle forces were estimated by the SLFBD performed at the L5-S1 level, using the EMG-assisted approach instead of an optimization algorithm [51,101]. For this purpose, the described measured normalized EMG data under the same task and loading were considered to drive the model [96]. The normalized EMG activity in each abdominal muscle (rectus abdominus, external oblique and internal oblique) was taken in the same way and varied from 12% (as measured) to 5%, or 0% while the activity in the local longissimus and iliocostalis lumbar muscles was assumed the same as that measured in the Multifidus (30%). The activity in quadratus lumborum (not measured in vivo) was taken as half of this latter value. The activities of the global longissimus and iliocostalis were taken as 30% and 24%, respectively, according to the in vivo measurements. The violation of equilibrium (IEV) was, subsequently, calculated at other levels.

Neglecting Translational DOF

The effect of neglecting axial and shear deformations, i.e., neglecting translational degrees-of-freedom at vertebral joints, considered in some earlier model investigations [35] on predictions, was evaluated by increasing the axial and shear stiffness of all intervertebral discs by a thousand-fold. This analysis was performed for a lifting task under a larger trunk flexion of $\sim 65^\circ$ with 180 N in the hands.

RESULTS

Wrapping of Global Muscles

As the trunk flexed from the upright standing position to a 46° forward flexion, the global muscles followed a curved path, while wrapping at different lumbar levels (Figure 4). For the case allowing a 10% reduction in LA, no wrapping, however, occurred at L1-L3 levels, as the LA distances at these levels did not fall below their corresponding critical values required for contact. The muscle and spinal compression forces at all levels

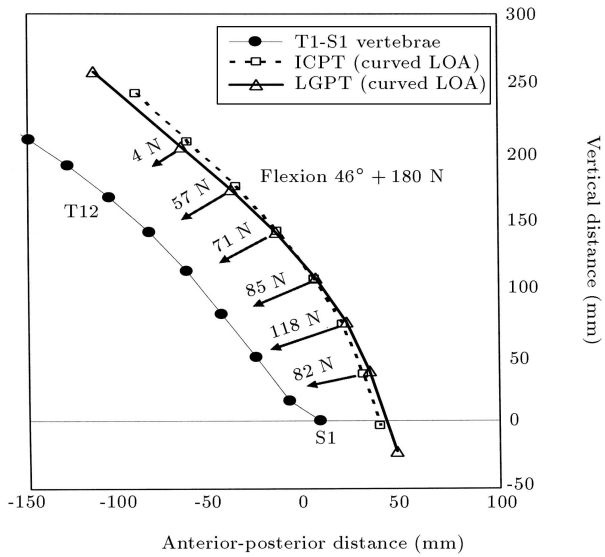

Figure 4. Magnitude and direction of wrapping contact forces acting on the spine due to wrapping of global muscles (Longissimus Thoracis pars thoracic, LGPT and Iliocostalis Lumborum pars thoracic, ICPT) for the case with no reduction in LAs from upright posture under trunk flexion of 46° with 180 N in hands.

substantially decreased, as the global ES took curved paths by wrapping around the T12-L5 levels, while preserving their LA distances (Table 2). In contrast, the segmental shear forces at distal L3-S1 levels increased in these cases (Table 1). A 10% reduction in the critical LA of wrapping global muscles increased compression forces at all levels. The wrapping of global muscles resulted in less muscle activity, as compared to the cases with straight muscles, as depicted in Figure 5, where the normalized active components of predicted muscle forces are compared with the normalized EMG data. When allowing for a 10% reduction in global muscle LAs, the muscle activities increased to magnitudes in-between the foregoing values for cases with either straight or curved global ES (Figure 5). Contact forces at the wrapping points generally increased from the upper vertebrae to the lower ones and, with the exception of that at the L5/S1 level, acted approximately perpendicular to the compressive axis of the spine (Figure 4).

Single-Level Free Body Diagram (SLFBD) Models

For the same spinal configuration, gravity/external load magnitudes/locations and passive ligamentous resistant moment as those used in the reference kinematics-driven model, muscle forces at both global and local levels substantially altered when calculated, based on the SLFBD model applied at different levels (Table 3 and Figure 6). Results indicate greater global

Table 2. Spinal loads (axial compression, shear and moment) for the lifting of 180 N at 46° trunk flexion without and with (no reduction or 10% reduction in lever arm) wrapping of global muscles.

		Flexion 46° + 180 N		
Disc	**Spinal Loads**	**No Wrapping (Straight LOA)**	**Wrapping (no Reduction in LA)**	**Wrapping (10% Reduction in LA)**
T12-L1	**S**[a]	490	269	358
	C[b]	1679	1287	1426
	M[c]	22	22	22
L1-L2	**S**	439	279	307
	C	2186	1540	1741
	M	28	27	27
L2-L3	**S**	202	187	124
	C	2606	1824	2023
	M	29	28	28
L3-L4	**S**	277	319	298
	C	2971	2202	2345
	M	25	23	24
L4-L5	**S**	73	247	240
	C	3250	2592	2724
	M	24	22	23
L5-S1	**S**	726	829	818
	C	3308	2751	2921
	M	27	27	26

(a) S: Local shear force (N), positive for anterior; (b) C: Local axial compression (N);

(c) M: Sagittal moment, positive for flexion (Nm).

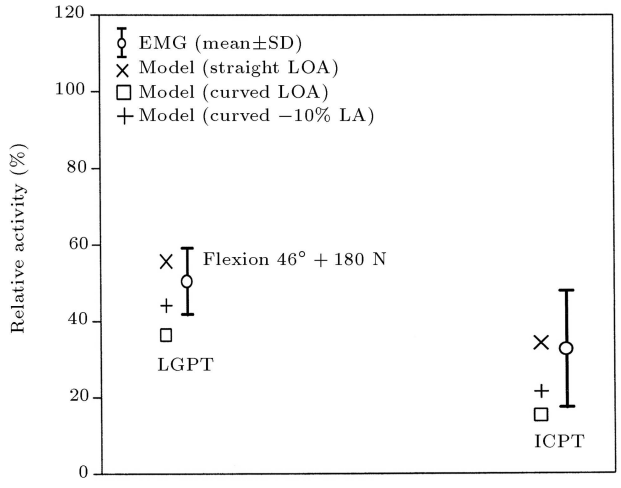

Figure 5. Normalized measured EMG activity (mean ± SD) of global muscles (Longissimus Thoracis pars thoracic, LGPT, and Iliocostalis Lumborum pars thoracic, ICPT) for flexion of 46° with 180 in hands. Predictions (normalized by 0.6×PCSA) have also been shown for the cases with straight LOA, curved LOA with no reduction in LA and curved LOA with a 10% reduction in LA for these muscles.

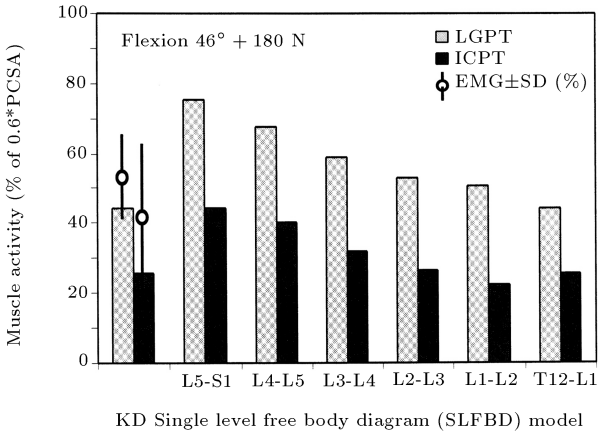

Figure 6. Normalized (to 0.6 times physiological cross sectional area) activity of global muscles (Longissimus Thoracis pars thoracic, LGPT, and Iliocostalis Lumborum pars thoracic, ICPT) for flexion of 46° with 180 in hands predicted using kinematics-driven (KD) approach and Single-Level Free Body Diagram (SLFBD) models considered at different T12-L1 through L5-S1 levels. Normalized measured EMG activity (mean ± SD) of these muscles is also shown.

Table 3. Predicted muscle forces for the lifting of 180 N at 46° trunk flexion using kinematics-driven approach as well as SLFBD models at different disc levels from L5-S1 through T12-L1 (forces in Iliopsoas muscles are zero in all SLFBD models and are not shown for the kinematics-based model).

Muscle	Upper Attach.	Muscle Forces on Each Side (N) for the Forward Flexed Posture						
		Kin.-Based	L5-S1 Cut	L4-L5 Cut	L3-L4 Cut	L2-L3 Cut	L1-L2 Cut	T12-L1 Cut
LGPT	**Thorax**	373	578	528	469	430	416	375
ICPT	**Thorax**	157	225	210	180	160	145	157
LGPL	**L1**	19	12	**11***	**11**	**11**	**11**	-
	L2	19	15	**11**	**11**	**11**	-	-
	L3	20	17	12	**12**	-	-	-
	L4	27	18	13	-	-	-	-
	L5	80	16	-	-	-	-	-
ICPL	**L1**	31	21	**19**	**19**	**19**	**19**	-
	L2	42	35	**27**	**27**	**27**	-	-
	L3	47	44	32	**29**	-	-	-
	L4	63	44	31	-	-	-	-
MF	**L1**	35	**26**	**26**	**26**	**26**	**26**	-
	L2	46	**31**	**31**	**31**	**31**	-	-
	L3	77	56	46	**34**	-	-	-
	L4	80	46	37	-	-	-	-
	L5	84	27	-	-	-	-	-
QL	**L1**	23	13	9	**7**	**7**	**7**	-
	L2	16	11	8	**7**	**7**	-	-
	L3	12	10	**7**	**7**	-	-	-
	L4	14	9	**6**	-	-	-	-

* Bold underlined numbers indicate the lower bound on muscle forces (i.e., only passive contribution).

thoracic muscle forces, whereas, generally, indicated smaller local lumbar muscle forces when comparing SLFBD models to kinematics-driven reference cases. In accordance with the constraint requirements in the kinematics-driven model, many local muscles in the forward flexed lifting task were assigned lower-bound forces, based on the muscle passive resistant force-length relationship and muscle instantaneous length (Table 1, underlined bold).

Local compression and shear forces at different spinal levels were also influenced when calculated based on SLFBD models; the former being smaller by as much as 7% compared with the reference kinematics-driven results (Table 4). The local shear force at the critical L5-S1 level, however, substantially increased by 19%, compared to the reference case when the SLFBD was performed at this level.

When comparing the results of SLFBD models against each other, there was a marked alteration in estimated muscle force, depending on the level considered (Table 3 and Figure 6). Furthermore, when applying the muscle forces, initially estimated by the SLFBD at the L5-S1 level as known forces, onto the SLFBD at remaining levels, the equilibrium of the sagittal moment was found to be grossly violated. The extent of error in the maintenance of equilibrium, identified as the Index of Equilibrium Violation (IEV), increased, as higher proximal levels were considered for this purpose and reached a maximum of 35% for the cut at the T12-L1 level (Figure 7). Similarly, axial compression forces at different levels altered substantially by as much as 38%, when calculated based on SLFBD models performed either at that level itself or at the L5-S1 level (Figure 8).

In order to satisfy equilibrium at the L5-S1 level, the EMG-assisted approach predicted gain factors of 0.36, 0.52 and 1.32 MPa, when no coactivity, a coactivity of 5% and a coactivity of 12% were considered for abdominal muscles, respectively. Moment equilibrium (IEV) was violated at the L4-L5 through T12-L1 levels by $\sim$ 5, 12, 24, 32 and 25%, respectively, when no coactivation was considered in the abdominals. These

Table 4. Predicted local spinal loads in the lifting of 180 N at 46° trunk flexion using kinematics-driven model as well as SLFBD models cut at different disc levels from L5-S1 through T12-L1.

Disc Level	Spinal Loads (N)													
	Kin.-Based		L5-S1 Cut		L4-L5 Cut		L3-L4 Cut		L2-L3 Cut		L1-L2 Cut		T12-L1 Cut	
	C[a]	S[b]	C	S	C	S	C	S	C	S	C	S	C	S
T12-L1	1426	358	-	-	-	-	-	-	-	-	-	-	1430	358
L1-L2	1741	307	-	-	-	-	-	-	-	-	1650	276	-	-
L2-L3	2023	124	-	-	-	-	-	-	1895	105	-	-	-	-
L3-L4	2345	298	-	-	-	-	2187	306	-	-	-	-	-	-
L4-L5	2724	240	-	-	2588	341	-	-	-	-	-	-	-	-
L5-S1	2921	818	2831	975	-	-	-	-	-	-	-	-	-	-

(a) C: Local axial compression (N); (b) S: Local shear force (N), positive in anterior direction.

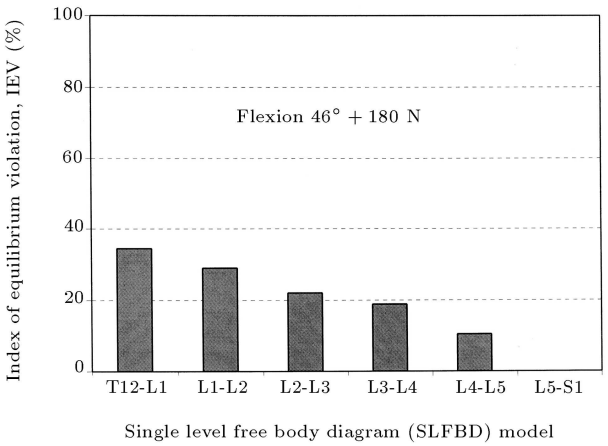

Figure 7. Index of Equilibrium Violation (IEV %) at different T12-L1 through L5-S1 levels when applying muscle forces calculated based on Single-Level Free Body Diagram (SLFBD) model at the L5-S1 level.

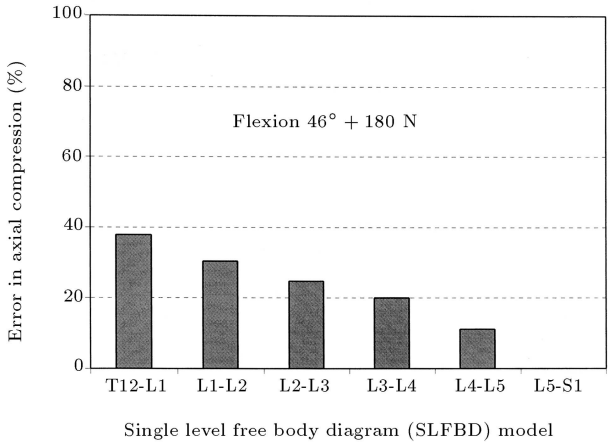

Figure 8. Relative error in axial compression forces estimated at different spinal levels when applying the muscle forces calculated by the Single-Level Free Body Diagram (SLFBD) model at the L5-S1 level compared to those calculated using SLFBD models directly at the level under consideration.

errors further increased in the presence of abdominal coactivities. To simultaneously satisfy moments at different levels, one would need to alter gains for the same muscles from one level to another; a remedy that would not make much sense.

Translational DOF

Both spinal compression and shear forces increased at all levels as the discs became excessively stiff in translational degrees-of-freedom (see Table 5). The influence of such assumption on the predicted shear forces was more substantial, reaching $\sim$ 18% at the critical L5-S1 level, while axial compression at different levels increased by $<$ 0%. Global muscle forces were also increased by $\sim$ 10%. The kinematics of the spine was also influenced, as the discs became very stiff in translational DOF; the vertebral translation at the T12 level increased by 1.2 mm in a horizontal forward direction, but decreased by 10.7 mm in an axial downward direction when compared to the reference case.

DISCUSSION

The kinematics-driven approach employed in this work yielded muscle forces and spinal loads that satisfied kinematics and kinetic conditions at various joints all along the spine, while considering both nonlinear material properties of the thoraco-lumbar motion segments and the wrapping of the trunk thoracic extensor muscles around the vertebrae. Predictions clearly indicated the importance of the proper consideration of: (a) Global extensor muscles as curved rather than straight lines, (b) Equilibrium equations at all levels rather than at a single level and (c) Translational degrees-of freedom at different levels, when attempting to estimate muscle forces and spinal loads in an isometric forward lifting task.

Table 5. Predicted spinal loads while neglecting translational Degrees-Of-Freedom (DOF) at vertebral joints compared to our reference case for the lifting of 180 N at 65° trunk flexion while considering wrapping of global muscles.

Level	Reference Case		No Translational DOF		Differences (%)	
	C[a]	S[b]	C	S	C	S
T12-L1	1398	488	1490	524	6.6	7.4
L1-L2	1804	450	1970	502	9.2	11.6
L2-L3	2182	236	2380	280	9.1	18.7
L3-L4	2592	394	2784	475	7.4	20.4
L4-L5	3116	264	3331	357	6.9	35.1
L5-S1	3247	869	3470	1027	6.9	18.2

(a) C: Local axial compression (N); (b) S: Local shear force (N), positive in anterior direction.

Wrapping of Global Muscles

A novel approach was introduced, in order to allow for global ES muscles with curved paths when simulating forward flexion tasks. Two cases of wrapping global muscles were considered, in which, as the spine flexed from the neutral standing posture, the critical LAs of global muscles required for wrapping either remained at their initial values during upright standing or were allowed to reduce by as much as 10% from these initial values. The hypothesis of this study regarding the importance of the wrapping of global muscles in large flexion postures was confirmed by predicting substantially smaller axial compression and muscle forces at all levels, with greater shear forces at lower levels (Table 2). The former predictions are expected, as larger LAs of global muscles in cases with wrapping muscles demand smaller muscle forces and, hence, smaller compression forces at different levels, while the latter predictions are due to the presence of wrapping contact forces. Wrapping contact forces, with the exception of that at the L5/S1 level, acted approximately perpendicular to the compressive axis of the spine (Figure 4), thus, primarily increasing anterior shear forces with a smaller effect on axial compression. The effect of contact forces on increasing the anterior shear force was especially obvious at the lower levels (L3-S1) (Table 2), while, at the upper levels, this effect disappeared, due to the more horizontal LOA of global muscles in cases with curved paths (Figure 4).

Some earlier biomechanical models [35] also considered curved pathways for extensor muscles that pass through several points at different vertebrae. These models, however, appear to have failed to account for reaction (contact) forces at these points of contact between muscles and vertebrae. These contact forces are due to changes in muscle orientation and generate moment, as well as shear/compression forces, which need to be considered in associated equilibrium equations at different levels. The simulation of wrapping without the proper consideration of these contact forces at the deformed configuration of the spine is not, hence, adequate adversely affecting the accuracy of the estimations.

Since the exact extent of the reduction in LAs of global muscles in flexion tasks remains unknown [74-76], a case was simulated allowing for a maximum of 10% reduction. This resulted in a considerable increase in spinal compression and muscle forces compared to the case in which no reduction in LA was allowed (Table 2 and Figure 5). Results also reiterate, in agreement with others [28,37,63], the sensitivity of the estimated spinal loads to anatomical assumptions, including the LOA and LA of global muscles.

To compare predictions with the present measurements, the EMG data were normalized with their measured MVC values, whereas the computed active muscle forces were normalized with their maximum value of 0.6*PCSA. Due to major concerns regarding the EMG data collected at the MVC tasks, the superficial EMG data collected at one level for each muscle, the maximum stress value of 0.6 MPa taken for the normalization of active muscle forces, the passive force-length relationship used for muscles in the model and the existence of EMG-force relationships, no attempt was made to adjust input data to arrive at specific activation values in better agreement with measurements. It is evident that changing the maximum active stress from 0.6 MPa to, for example, 0.5 MPa or, inversely, to 0.7 MPa, while remaining still in the range of reported values in the literature, would shift all predicted values in Figure 5 substantially upward or downward, respectively.

Single-Level Free Body Diagram (SLFBD) Models

This part of the work is aimed at quantifying the extent to which the muscle forces, spinal loads and equilibrium requirements at different levels are influenced when considering a Single-Level Free Body Diagram (SLFBD) equilibrium at a specific spinal level, or as

it alters from one level to another. Such models, driven either by optimization cost functions or by EMG data, are widely employed in biomechanical model investigations of the human spine, in order to estimate muscle forces and spinal loads [38,50,62-66]. The emphasis in this work is on the reliability of SLFBD model predictions. The kinematics-driven model was primarily performed to obtain the deformed configurations, external/gravity load magnitudes/positions and passive resistant loads required in SLFBD models. The results of this investigation confirmed the hypotheses of the study in that the SLFBD models yield results that grossly violate the equilibrium at levels other than the one considered in the model and that the extent of such violations, as well as the magnitude of muscle forces and spinal loads, alters as a function of the disc level considered and most likely of the task simulated. Results also demonstrated that the predictions of SLFBD models are markedly level dependent; that is, they significantly alter when different levels are used for the sake of the calculation of muscle forces and internal loads.

In the kinematics-driven model, the optimization algorithm was employed at all levels, separately one from another, in order to partition the required moment calculated for a given prescribed rotation in between muscles that are attached only to the level under consideration. The remaining muscles not attached to this specific level, either crossing over or attached to lower ones, would, therefore, be absent in the equilibrium equations under investigation. The consideration of all levels, one by one, would, therefore, yields all unknown muscle forces under the given kinematics and external/gravity loads. On the contrary, in the SLFBD model, the forces in all muscles passing through the cross-section in question, inserted or not into that specific level, were treated as the unknowns in a single equation of equilibrium. For this reason and since identical data were shared, almost the same results were obtained in both reference and single-level models for global extensor muscle forces and local spinal loads at the T12-L1 level, when the FBD was considered at the T12-L1 level (Tables 3 and 4, Figure 6). Substantial differences in global muscle forces were, however, found when the lower levels were considered in the SLFBD model.

Muscle forces calculated at one level, irrespective of the method used, must satisfy equilibrium when applied at remaining levels in order to be reliable. The index of violation in the moment equation of equilibrium at different levels (Figure 7), indicating the error in estimated muscle forces, based on the SLFBD at the L5-S1 level, increased proximally from the L4-L5 level to its maximum of 35% at the T12-L1 level. This error clearly lends support to the fact that equilibrium equations at all levels and in all directions should be treated simultaneously, as is undertaken in the kinematics-driven finite element model, and not in isolation from each other, as in popular SLFBD models. The substantial differences between muscle forces, when calculated based on the SLFBD at different levels (Table 3 and Figure 6), also suggest the major shortcoming in such model studies. It should be reiterated that, predicted in this study, large differences between the results of SLFBD models, both between themselves, depending on the level considered and the kinematics-driven results occurred despite using identical deformed configurations (ligamentous spine and muscles), external/gravity magnitudes/locations, the passive resistant moment of the ligamentous spine, the passive properties of muscles and the optimization algorithm of the sum of the cubed muscle stresses. It is evident that, had the muscle forces estimated from different SLFBD models been applied as external loads on the spine, substantially different deformed (and possibly unstable) configurations would have been generated, depending on the level considered in the SLFBD. The resulting spinal configurations would also be quite different from the initial configuration considered in SLFBD calculations.

Regardless of the method used to resolve the redundancy problem and partition the net moment among muscles, i.e. optimization methods or the EMG-assisted approach, the equilibrium was not satisfied simultaneously at levels other than the one used to estimate muscle forces. These findings further confirm the shortcoming of SLFBD models. Comparison of the predicted results of the kinematics-driven model with SLFBD models, regardless of the method used to tackle the redundancy, also demonstrated that the differences in the computed axial compression force at different levels remained $< 7\%$ (Table 4) being much lower than those for shear and muscle forces. In other words, the axial compression force appears to be less sensitive to shortcomings in SLFBD models. Earlier investigations have also found that the effect of different optimization cost functions (especially nonlinear ones) on the estimated axial compression, in both kinematics-driven [102] and SLFBD [63] models, is not significant. For this reason, and due to the relative ease of SLFBD applications, one may argue that such SLFBD models could be carried out with the specific objective of estimating only local compression loads on the spine, not the shear forces and muscle activation levels.

Translational DOF

Results suggested the importance of an accurate representation of motion segments in the model of the passive ligamentous spine. The simulation of discs with no horizontal and axial translations, as undertaken in some earlier studies (similar to pin joints with rota-

tional springs only) [35], would, hence, yield erroneous results, as far as muscle forces and spinal loads are concerned. The kinematics of the spine would also be influenced by such simplifying assumptions.

Finally, in this work, using the kinematics-driven approach, the crucial effects of the proper consideration of global muscles with curved paths and of spinal segments with translational degrees-of-freedom were demonstrated in the biomechanical model studies of an isometric lifting task. Moreover, substantial errors were identified in the results of the SLFBD models, suggesting the importance of the simultaneous consideration of equilibrium at all levels when attempting to estimate muscle forces and spinal loads.

ACKNOWLEDGMENT

The work is supported by the Natural Sciences and Engineering Research Council of Canada (NSERC-Canada).

REFERENCES

1. Ashton-Miller, J.A. and Schultz, A.B. "Biomechanics of the human spine", *Basic Orthopedic Biomechanics*, 2nd Ed., Philadelphia, Lippincott-Raven, pp 353-393 (1997).
2. Frymoyer, J. "The magnitude of the problem", In *The Lumbar Spine*, Philadelphia: WB Saunders, pp 8-15 (1996)
3. Nachemson, A. "Newest knowledge of low back pain, a critical look", *Clin Orthop Relat Res.*, **279**, pp 8-20 (1992).
4. Praemer, A., Furner, S. and Rice, D.P. "Musculoskeletal conditions in the united states", Park Ridge, III: American Academy of Orthopaedic Surgeons, pp 23-33 (1992).
5. Webster, B.S. and Snook, S.H. "The cost of 1989 workers' compensation low back pain claims", *Spine*, **19**, pp 1111-5 (1994).
6. Damkot, D.K., Pope, M.H., Lord, J. and Frymoyer, J.W. "The relationship between work history, work environment and low-back pain in men", *Spine*, **9**, pp 395-9 (1984).
7. Marras, W.S., Lavender, S.A., Leurgans, S.E., Fathallah, F.A., Ferguson, S.A., Allread, W.G. and Rajulu, S.L. "Biomechanical risk factors for occupationally related low back disorders", *Ergonomics*, **38**, pp 377-410 (1995).
8. Kelsey, J.L., Githens, P.B., White, A.A. 3rd, Holford, T.R., Walter, S.D., O'Connor, T., Ostfeld, A.M., Weil, U., Southwick, W.O. and Calogero, J.A. "An epidemiologic study of lifting and twisting on the job and risk for acute prolapsed lumbar intervertebral disc", *J. Orthop. Res.*, **2**, pp 61-6 (1984).
9. Hoogendoorn, W.E., Bongers, P.M., de Vet, H.C., Douwes, M., Koes, B.W., Miedema, M.C., Ariens, G.A. and Bouter, L.M "Flexion and rotation of the trunk and lifting at work are risk factors for low back pain: Results of a prospective cohort study", *Spine*, **25**, pp 3087-92 (2000).
10. Troup, J.D., Martin, J.W. and Lloyd, D.C. "Back pain in industry. A prospective survey", *Spine*, **6**, pp 61-9 (1981).
11. Varma, K.M. and Porter, R.W. "Sudden onset of back pain", *Eur. Spine J.*, **4**, pp 145-7 (1995).
12. Andersson, G.B. "Epidemiologic aspects on low-back pain in industry", *Spine*, **6**, pp 53-60 (1981).
13. Natinal Institute for Occupational Safety and Health (NIOSH),*Musculoskeletal Disorders and Workplace Factors*, U.S. Dept. of Health and Human Services (1997).
14. Ferguson, S.A. and Marras, W.S. "A literature review of low back disorder surveillance measures and risk factors", *Clin Biomech.*, **12**, pp 211-226 (1997).
15. Burdorf, A. and Sorock, G. "Positive and negative evidence of risk factors for back disorders", *Scand J. Work Environ Health*, **23**, pp 243-56 (1997).
16. Frank, J.W., Kerr, M.S., Brooker, A.S., DeMaio, S.E., Maetzel, A., Shannon, H.S., Sullivan, T.J., Norman, R.W. and Wells, R.P. "Disability resulting from occupational low back pain. Part I: What do we know about primary prevention? A review of the scientific evidence on prevention before disability begins", *Spine*, **21**, pp 2908-17 (1996).
17. Nachemson, A. "Disc pressure measurements", *Spine*, **6**, pp 93-97 (1981).
18. Wilke, H.J., Neef, P., Caimi, M., Hoogland, T. and Claes, L.E. "New in vivo measurements of pressures in the intervertebral disc in daily life", *Spine*, **24**, pp 755-763 (1999).
19. Davis, P.R. "The use of intra-abdominal pressure in evaluating stresses on the lumbar spine", *Spine*, **6**, pp 90-2 (1981).
20. van Dieen, J.H. and Toussaint, H.M. "Spinal shrinkage as a parameter of functional load", *Spine*, **18**, pp 1504-14 (1993).
21. McGill, S.M., van Wijk, M.J., Axler, C.T. and Gletsu, M. "Studies of spinal shrinkage to evaluate low-back loading in the workplace", *Ergonomics*, **39**, pp 92-102 (1996).
22. van Dieen, J.H., Hoozemans, M.J. and Toussaint, H.M. "Stoop or squat: A review of biomechanical studies on lifting technique", *Clin Biomech.*, **14**, pp 685-96 (1999).
23. Reeves, N.P. and Cholewicki, J. "Modeling the human lumbar spine for assessing spinal loads, stability, and risk of injury", *Crit. Rev. Biomed. Eng.*, **31**, pp 73-139 (2003).
24. Chaffin, D.B. "A computerized biomechanical model-development of and use in studying gross body actions", *J. Biomech.*, **2**, pp 429-41 (1969).

25. Leskinen, T.P., Stalhammar, H.R., Kuorinka, I.A. and Troup, J.D. "The effect of inertial factors on spinal stress when lifting", *Eng. Med.*, **12**, pp 87-9 (1983).
26. de Looze, M.P., Visser, B., Houting, I., van Rooy, M.A., van Dieen, J.H. and Toussaint, H.M. "Weight and frequency effect on spinal loading in a bricklaying task", *J. Biomech.*, **29**, pp 1425-33 (1996).
27. Morris, J., Lucas, D.B. and Bresler, B. "Role of the trunk in stability of the spine", *J. Bone Joint Surg.*, **43A**, pp 327-351 (1961).
28. van Dieen, J.H. and de Looze, M.P. "Sensitivity of single-equivalent trunk extensor muscle models to anatomical and functional assumptions", *J. Biomech.*, **32**, pp 195-8 (1999).
29. Bogduk, N., Macintosh, J.E. and Pearcy, M.J. "A universal model of the lumbar back muscles in the upright position", *Spine*, **17**, pp 897-913 (1992).
30. Daggfeldt, K. and Thorstensson, A. "The mechanics of back-extensor torque production about the lumbar spine", *J. Biomech.*, **36**, pp 815-25 (2003).
31. Jorgensen, M.J., Marras, W.S., Granata, K.P. and Wiand, J.W. "MRI-derived moment-arms of the female and male spine loading muscles", *Clin. Biomech.*, **16**, pp 182-93 (2001).
32. McGill, S.M., *Low Back Disorders, Evidence-Based Prevention and Rehabilitation*, 1st Ed., Human Kinetics Publishers (2002).
33. Stokes, I.A. and Gardner-Morse, M. "Quantitative anatomy of the lumbar musculature", *J. Biomech.*, **32**, pp 311-316 (1999).
34. Wood, S., Pearsall, D.J., Ross, R. and Reid, J.G. "Trunk muscle parameters determined from MRI for lean to obese males", *Clin. Biomech.*, **11**, pp 139-144 (1996).
35. Cholewicki, J. and McGill, S.M. "Mechanical stability of the in vivo lumbar spine: Implications for injury and chronic low back pain", *Clin. Biomech.*, **11**, pp 1-15 (1996).
36. Han, J.S., Ahn, J.Y., Goel, V.K., Takeuchi, R. and McGowan, D. "CT-based geometric data of human spine musculature. Part I. Japanese patients with chronic low back pain", *J. Spinal Disord*, **5**, pp 448-58 (1992).
37. Nussbaum, M.A., Chaffin, D.B. and Rechtien, C.J. "Muscle lines-of-action affect predicted forces in optimization-based spine muscle modeling", *J. Biomech*, **28**, pp 401-9 (1995).
38. Schultz, A., Andersson, G., Ortengren, R., Haderspeck, K., Ortengren, R., Nordin, M. and Bjork, R. "Analysis and measurement of lumbar trunk loads in tasks involving bends and twists", *J. Biomech*, **15**, pp 669-75 (1982).
39. Seireg, A. and Arvikar, R.J. "A mathematical model for evaluation of forces in lower extremities of the musculo-skeletal system", *J. Biomech*, **6**, pp 313-26 (1973).
40. Yettram, A.L. and Jackman, M.J. "Structural analysis for the forces in the human spinal column and its musculature", *J. Biomed. Eng.*, **4**, pp 118-24 (1982).
41. Zetterberg, C., Andersson, G.B. and Schultz, A.B. "The activity of individual trunk muscles during heavy physical loading", *Spine*, **12**, pp 1035-40 (1987).
42. Crowninshield, R.D. and Brand, R.A. "A physiologically based criterion of muscle force prediction in locomotion", *J. Biomech.*, **14**, pp 793-801 (1981).
43. Hughes, R.E., Chaffin, D.B., Lavender, S.A. and Andersson, G.B. "Evaluation of muscle force prediction models of the lumbar trunk using surface electromyography", *J. Orthop Res.*, **12**, pp 689-98 (1994).
44. Hughes, R.E., Bean, J.C. and Chaffin, D.B. "Evaluating the effect of co-contraction in optimization models", *J. Biomech.*, **28**, pp 875-8 (1995).
45. Shirazi-Adl, A. and Parnianpour, M. "Finite element model studies in lumbar spine biomechanics", *Computer Techniques and Computational Methods in Biomechanics*, New York, CRC press, pp 1-36 (2001).
46. Herzog, W. "Sensitivity of muscle force estimations to changes in muscle input parameters using nonlinear optimization approaches", *J. Biomech, Eng.*, **114**, pp 267-8 (1992).
47. Prilutsky, B.I., Isaka, T., Albrecht, A.M. and Gregor, R.J. "Is coordination of two-joint leg muscles during load lifting consistent with the strategy of minimum fatigue?", *J. Biomech.*, **31**, pp 1025-34 (1998).
48. van Bolhuis, B.M. and Gielen, C.C. "A comparison of models explaining muscle activation patterns for isometric contractions", *Biol. Cybern.*, **81**, pp 249-61 (1999).
49. Stokes, I.A. and Gardner-Morse, M. "Lumbar spinal muscle activation synergies predicted by multicriteria cost function", *J. Biomech.*, **34**, pp 733-740 (2001).
50. McGill, S.M. and Norman, R.W. "Partitioning of the L4-L5 dynamic moment into disc, ligamentous, and muscular components during lifting", *Spine*, **11**, pp 666-78 (1986).
51. Marras, W.S. and Granata, K.P. "The development of an EMG-assisted model to assess spine loading during whole-body free-dynamic lifting", *Journal of Electromyography and Kinesiology*, **7**, pp 259-268 (1997).
52. Gagnon, D., Lariviere, C. and Loisel, P. "Comparative ability of EMG, optimization, and hybrid modelling approaches to predict trunk muscle forces and lumbar spine loading during dynamic sagittal plane lifting", *Clin Biomech.*, **16**, pp 359-72 (2001).
53. Moseley, G.L., Hodges, P.W. and Gandevia, S.C. "Deep and superficial fibers of the lumbar multifidus muscle are differentially active during voluntary arm movements", *Spine*, **27**, pp E29-36 (2002).

54. McGill, S., Juker, D. and Kropf, P. "Appropriately placed surface EMG electrodes reflect deep muscle activity (psoas, quadratus lumborum, abdominal wall) in the lumbar spine", *J. Biomech.*, **29**, pp 1503-7 (1996).
55. Strohl, K.P., Mead, J., Banzett, R.B., Loring, S.H. and Kosch, P.C. "Regional di.erences in abdominal muscle activity during various maneuvers in humans", *J. Appl. Physiol.*, **51**, pp 1471-1476 (1981).
56. Davis, J.R. and Mirka, G.A. "Transverse-contour modeling of trunk muscle-distributed forces and spinal loads during lifting and twisting", *Spine*, **25**, pp 180-189 (2000).
57. Mirka, G., Kelaher, D., Baker, A., Harrison, A. and Davis, J. "Selective activation of the external oblique musculature during axial torque production", *Clin Biomech.*, **12**, pp 172-180 (1997).
58. Hodges, P., Cresswell, A. and Thorstensson, A. "Preparatory trunk motion accompanies rapid upper limb movement", *Exp. Brain Res.*, **124**, pp 69-79 (1999).
59. van Dieen, J.H. and Kingma, I. "Effects of antagonistic co-contraction on differences between electromyography based and optimization based estimates of spinal forces", *Ergonomics*, **48**, pp 411-26 (2005).
60. Calisse, J., Rohlmann, A. and Bergmann, G. "Estimation of trunk muscle forces using the finite element method and in vivo loads measured by telemeterized internal spinal fixation devices", *J. Biomech.*, **32**, pp 727-31 (1999).
61. Cholewicki, J. and McGill, S.M. "EMG assisted optimization: A hybrid approach for estimating muscle forces in an indeterminate biomechanical model", *J. Biomech.*, **27**, pp 1287-9 (1994).
62. Cholewicki, J., McGill, S.M. and Norman, R.W. "Comparison of muscle forces and joint load from an optimization and EMG assisted lumbar spine model: Towards development of a hybrid approach", *J. Biomech.*, **28**, pp 321-31 (1995).
63. Parnianpour, M., Wang, J.L., Shirazi-Adl, A., Sparto, P. and Wilke, H.J. "The effect of variations in trunk models in predicting muscle strength and spinal loads", *Journal of Musculoskeletal Research*, **1**, pp 55-69 (1997).
64. van Dieen, J.H., Kingma, I. and van Der Bug, P. "Evidence for a role of antagonistic cocontraction in controlling trunk stiffness during lifting", *J. Biomech.*, **36**, pp 1829-36 (2003).
65. Granata, K.P., Lee, P.E. and Franklin, T.C. "Cocontraction recruitment and spinal load during isometric trunk flexion and extension", *Clin Biomech.*, **20**, pp 1029-37 (2005).
66. Marras, W.S., Parakkat, J., Chany, A.M., Yang, G., Burr, D. and Lavender, S.A. "Spine loading as a function of lift frequency, exposure duration, and work experience", *Clin Biomech.*, **21**, pp 345-52 (2006).
67. Stokes, I.A. and Gardner-Morse, M. "Lumbar spine maximum efforts and muscle recruitment patterns predicted by a model with multijoint muscles and joints with stiffness", *J. Biomech.*, **28**, pp 173-86 (1995).
68. Dietrich, M., Kedzior, K. and Zagrajek, T. "A biomechanical model of the human spinal system", *Proceedings of the Institution of Mechanical Engineers*, Part H, **205**, pp 19-26 (1991).
69. Gardner-Morse, M., Stokes, I.A.F. and Laible, J.P. "Role of muscles in lumbar spine stability in maximum extension efforts", *Journal of Orthopaedic Research*, **13**, pp 802-808 (1995).
70. Gardner-Morse, M. and Stokes, I.A.F. "The effects of abdominal muscle coactivation on lumbar spine stability", *Spine*, **23**, pp 86-92 (1998).
71. Patwardhan, A.G., Havey, R.M., Carandang, G., Simonds, J., Voronov, L.I., Ghanayem, A.J., Meade, K.P., Gavin, T.M. and Paxinos, O. "Effect of compressive follower preload on the flexion-extension response of the human lumbar spine", *Journal of Orthopaedic Research*, **21**, pp 540-6 (2003).
72. Shirazi-Adl, A. "Analysis of large compression loads on lumbar spine in flexion and in torsion using a novel wrapping element", *J. Biomech.*, **39**, pp 267-75 (2006).
73. Stokes, I.A. and Gardner-Morse, M. "Spinal stiffness increases with axial load: another stabilizing consequence of muscle action", *J. Electromyogr Kinesiol*, **13**, pp 397-402 (2003).
74. Jorgensen, M.J., Marras, W.S., Gupta, P. and Waters, T.R. "Effect of torso flexion on the lumbar torso extensor muscle sagittal plane moment arms", *The Spine J.*, **3**, pp 363-9 (2003).
75. Macintosh, J.E., Bogduk, N. and Pearcy, M.J. "The effects of flexion on the geometry and actions of the lumbar erector spinae", *Spine*, **18**, pp 884-93 (1993).
76. Tveit, P., Daggfeldt, K., Hetland, S. and Thorstensson, A. "Erector spinae lever arm length variations with changes in spinal curvature", *Spine*, **19**, pp 199-204 (1994).
77. McGill, S.M., Hughson, R.L. and Parks, K. "Changes in lumbar lordosis modify the role of the extensor muscles", *Clin Biomech.*, **15**, pp 777-80 (2000).
78. McGill, S.M. "Electromyographic activity of the abdominal and low back musculature during the generation of isometric and dynamic axial trunk torque: Implications for lumbar mechanics", *Journal of Orthopaedic Research*, **9**, pp 91-103 (1991).
79. O'Sullivan, P.B., Grahamslaw, K.M., Kendell, M., Lapenskie, S.C., Moller, N.E. and Richards, K.V. "The effect of different standing and sitting postures on trunk muscle activity in a pain-free population", *Spine*, **27**, pp 1238-1244 (2002).
80. Sparto, P.J. and Parnianpour, M. "Estimation of trunk muscle forces and spinal loads during fatiguing repetitive trunk exertions", *Spine*, **23**, pp 423-429 (1998).

81. Granata, K.P. and Sanford, A.H. "Lumbar-pelvic coordination is influenced by lifting task parameters", *Spine*, **25**, pp 1413-8 (2000).
82. Kiefer, A., Shirazi-Adl, A. and Parnianpour, M. "Synergy of human spine in neutral postures", *European Spine Journal*, **7**, pp 471-479 (1998).
83. Pop, D.G. "Analyse non linéaire par éléments finis du système actif passif de la colonne vertébrale humaine", *M.Sc.A. Dissertation Génie mécanique, École Polytechnique*, Montréal, Québec (2001).
84. Shirazi-Adl, A., Sadouk, S., Parnianpour, M., Pop, D. and El-Rich, M. "Muscle force evaluation and the role of posture in human lumbar spine under compression", *European Spine Journal*, **11**, pp 519-526 (2002).
85. Shirazi-Adl, A., El-Rich, M., Pop, D.G. and Parnianpour, M. "Spinal Muscle forces, internal loads and stability in standing under various postures and loads: Applications of kinematics-based algorithm", *European Spine Journal*, **14**, pp 381-92 (2005).
86. Oxland, T., Lin, R.M. and Panjabi, M. "Three-dimensional mechanical properties of the thoracolumbar junction", *Journal of Orthopaedic Research*, **10**, pp 573-580 (1992).
87. Yamamoto, I., Panjabi, M., Crisco, T. and Oxland, T. "Three-dimensional movements of the whole lumbar spine and lumbosacral joint", *Spine*, **14**, pp 1256-1260 (1989).
88. Shirazi-Adl, A., Ahmed, A.M. and Shrivastava, S.C. "A finite element study of a lumbar motion segment subjected to pure sagittal plane moments", *Journal of Biomechanics*, **19**, pp 331-350 (1986).
89. Shirazi-Adl, A., Ahmed, A.M. and Shrivastava, S.C. "Mechanical response of a lumbar motion segment in axial torque alone and combined with compression", *Spine*, **11**, pp 914-927 (1986).
90. Pearsall, D.J. "Segmental inertial properties of the human trunk as determined from computer tomography and magnetic resonance imagery", PhD Thesis, Queen's University, Kingston, Ontario (1994).
91. Takashima, S.T., Singh, S.P., Haderspeck, K.A. and Schultz, A.B. "A model for semi-quantitative studies of muscle actions", *Journal of Biomechanics*, **12**, pp 929-939 (1979).
92. Dvorak, J., Panjabi, M.M., Chang, D.G., Theiler, R. and Grob, D. "Functional radiographic diagnosis of the lumbar spine: Flexion-extension and lateral bending", *Spine*, **16**, pp 562-71 (1991).
93. Pearcy, M., Portek, I. and Shepherd, J. "Three-dimensional x-ray analysis of normal movement in the lumbar spine", *Spine*, **9**, pp 294-7 (1984).
94. Plamondon, A., Gagnon, M. and Maurais, G. "Application of a stereoradiographic method for the study of intervertebral motion", *Spine*, **13**, pp 1027-32 (1988).
95. Potvin, J.R., McGill, S.M. and Norman, R.W. "Trunk muscle and lumbar ligament contributions to dynamic lifts with varying degrees of trunk flexion", *Spine*, **16**, pp 1099-107 (1991).
96. El-Rich, M., Shirazi-Adl, A. and Arjmand, N. "Muscle activity, internal loads and stability of the human spine in standing postures: Combined model-in vivo studies", *Spine*, **29**, pp 2633-42 (2004).
97. Davis, J., Kaufman, K.R. and Lieber, R.L. "Correlation between active and passive isometric force and intramuscular pressure in the isolated rabbit tibialis anterior muscle", *Journal of Biomechanics*, **36**, pp 505-12 (2003).
98. Arjmand, N. and Shirazi-Adl, A. "Model and in vivo studies on human trunk load partitioning and stability in isometric forward flexions", *J. Biomech.*, **39**, pp 510-21 (2006).
99. Shirazi-Adl, A. "Nonlinear finite element analysis of wrapping uniaxial elements", *Computers & Structures*, **32**, pp 119-123 (1989).
100. Shirazi-Adl, A. and Parnianpour, M. "Load-bearing and stress analysis of the human spine under a novel wrapping compression loading", *Clin Biomech*, **15**, pp 718-25 (2000).
101. McGill, S.M. "A myoelectrically based dynamic three-dimensional model to predict loads on lumbar spine tissues during lateral bending", *Journal of Biomechanics*, **25**, pp 395-414 (1992).
102. Arjmand, N. and Shirazi-Adl, A. "Sensitivity of kinematics-based model predictions to optimization criteria in static lifting tasks", *Medical Engineering & Physics*, **28**, pp 504-514 (2006).